

# Solar wind charge exchange and local hot bubble X-ray emission with the DXL sounding rocket experiment

M. Galeazzi<sup>1,\*</sup>, M.R. Collier<sup>2</sup>, T. Cravens<sup>3</sup>, D. Koutroumpa<sup>4</sup>, K.D. Kuntz<sup>5</sup>, S. Lepri<sup>6</sup>, D. McCammon<sup>7</sup>, F. S. Porter<sup>2</sup>, K. Prasai<sup>1</sup>, I. Robertson<sup>3</sup>, S. Snowden<sup>2</sup>, N.E. Thomas<sup>2</sup>, and Y. Uprety<sup>1</sup>

<sup>1</sup> University of Miami, Department of Physics, 1320 Campo Sano Dr., Coral Gables, FL 33146, USA

<sup>2</sup> NASA/Goddard Space Flight Center, Greenbelt, MD 20771, USA

<sup>3</sup> University of Kansas, Department of Physics and Astronomy, 1251 Wescoe Hall Dr., Lawrence, KS 66045, USA

<sup>4</sup> LATMOS-IPSL/CNRS, 11 Boulevard d'Alembert, 78280 Guyancourt, France

<sup>5</sup> The Johns Hopkins University, The Henry A. Rowland Department of Physics and Astronomy, Baltimore, MD 21218, USA

<sup>6</sup> University of Michigan, 2455 Hayward St., Ann Arbor, MI 48109, USA

<sup>7</sup> University of Wisconsin, Department of Physics, 1150 University Ave., Madison, WI 53706, USA

Received 2012 Mar 2, accepted 2012 Mar 8

Published online 2012 Apr 20

**Key words** instrumentation: detectors – interplanetary medium – ISM: bubbles – solar wind – X-rays: ISM

The Diffuse X-ray emission from the Local Galaxy (DXL) sounding rocket is a NASA approved mission with a scheduled first launch in December 2012. Its goal is to identify and separate the X-ray emission of the solar wind charge exchange (SWCX) from that of the local hot bubble (LHB) to improve our understanding of both. To separate the SWCX contribution from the LHB, DXL will use the SWCX signature due to the helium focusing cone at  $l = 185^\circ$ ,  $b = -18^\circ$ . DXL uses large area proportional counters, with an area of 1000 cm<sup>2</sup> and grasp of about 10 cm<sup>2</sup> sr both in the 1/4 and 3/4 keV bands. Thanks to the large grasp, DXL will achieve in a 5-minute flight what cannot be achieved by current and future X-ray satellites.

© 2012 WILEY-VCH Verlag GmbH & Co. KGaA, Weinheim

## 1 Introduction

In Solar Wind Charge eXchange (SWCX), highly ionized ions in the solar wind collide with neutral atoms picking up an electron in an excited state. The electron then decays producing UV and X-ray emission. SWCX was originally discovered from observations of comets, where solar wind would “charge exchange” with the neutrals in the comet (Cravens 1997). It is now believed that solar wind also “charge exchanges” with neutrals in the Earth’s exosphere (magnetosheath SWCX) (Cravens 2001, Robertson and Cravens 2003a,b) and with interstellar neutrals in the solar system (heliospheric SWCX) (Cox 1998).

It has been suggested that SWCX emission may be responsible for all of the “local flux” observed at 1/4 keV in the galactic plane (Lallement 2004a,b) and that much of the observed 3/4 keV emission may also originate from SWCX (Koutroumpa et al. 2007), affecting our understanding of the physical parameters of the interstellar medium and the halo of the Milky Way.

The SWCX spectrum is dominated by characteristic line emission that is very difficult to separate from the presumably thermal emission of other galactic diffuse X-ray components, such as local hot bubble (LHB) and halo emission (e.g., McCammon et al. 2002; Galeazzi et al. 2007; Gupta

et al. 2009). It should, however, be possible to separate it by looking at its spatial and temporal signatures. The slowest time-varying, and thus most troublesome, heliospheric component of the SWCX emission originates in the interplanetary medium and should show a significant geometric variation due to the focusing of interplanetary helium. Interstellar neutrals flow through the solar system due to the motion of the heliosphere through the local interstellar cloud. Gravity significantly affects helium trajectories which execute Keplerian orbits and form a “focusing cone” downstream of the Sun centered at  $\sim 6^\circ$  below the ecliptic plane. This results in a localized downstream enhancement of helium which has the direct effect of increasing the SWCX X-ray emission. By scanning the sky through the focusing cone, the spatial signature of the SWCX can be identified, allowing a separation and subsequent investigation of LHB and SWCX emission.

While there are well-defined models for SWCX emission from the heliosphere, testing them is problematic. Koutroumpa et al. (2007), using a self-consistent model of the heliospheric SWCX emission, managed to associate observed discrepancies in XMM-Newton and Suzaku observations separated by several years with solar cycle-scale variations of the heliospheric SWCX emission. A recent paper (Snowden et al. 2009) was successful in using an XMM-Newton observation to test a model (Robertson &

\* Corresponding author: galeazzi@physics.miami.edu

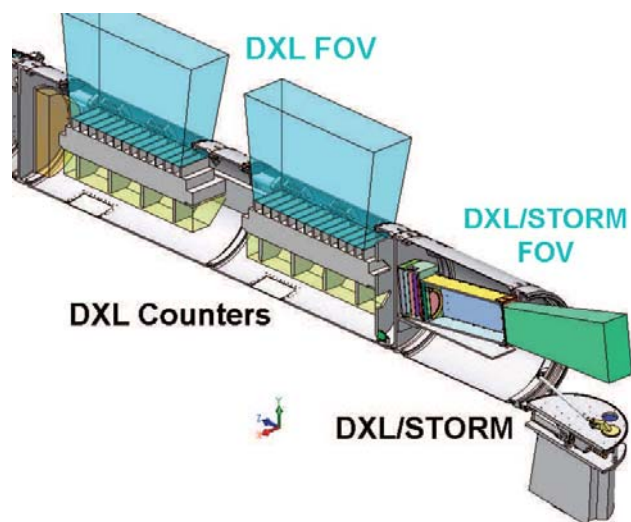


**Fig. 1** (online colour at: [www.an-journal.org](http://www.an-journal.org)) Cross section of the experimental section of the DXL payload with the DXL and DXL/STORM detectors and their field of view (FOV).

Cravens 2003a) for emission from the near-Earth environment. Koutroumpa et al. (2009) uses a different series of XMM-Newton observations to search for SWCX emission from the He focusing cone. They were relatively successful, but the detection was at a marginal level due to the short exposures and higher backgrounds experienced by XMM-Newton.

## 2 DXL concept

A cross section of the DXL payload experimental section (Galeazzi et al. 2011) is shown in Fig. 1. The main instrument is the DXL detector, which is composed of two large area ( $500 \text{ cm}^2$  each at 1 keV) thin window proportional counters that provide excellent counting statistics when scanning the sky through the He focusing cone in the limited observing time of a sounding rocket flight. The figure of merit to quantify the performance of a detector such as DXL is the grasp, i.e., the product of the effective area times solid angle. The grasp and effective area of DXL as a function of energy are shown in Fig. 2. In particular, the DXL grasp at 0.65 keV, the O VIII energy, is about  $7.5 \text{ cm}^2 \text{ sr}$  ( $600 \text{ cm}^2$  area,  $6.5^\circ \times 6.5^\circ$  FOV). By comparison, XMM-Newton has a grasp about 150 times smaller and Suzaku about 2000 times smaller, requiring 40 000 s and 600 000 s of observing time respectively, to obtain at 0.65 keV comparable science results as 5 minutes with DXL. At lower energy, where the SWCX contribution becomes more important, the situation is much better for DXL as the effective area for current flight observatories drops well below  $100 \text{ cm}^2$ , making any SWCX science there essentially impossible. Future calorimetric missions such as Astro-H and Athena will fare even worse, due their small field of view, while eROSITA is ex-

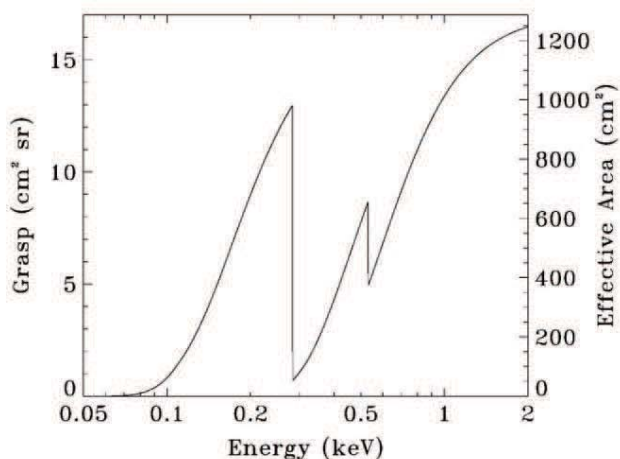


**Fig. 2** Effective area and grasp of the DXL payload below 2 keV.

pected to have a grasp about 50 times smaller than DXL and will be used primarily in survey mode.

In addition to the primary DXL instrument, a second instrument, DXL/STORM, will also be mounted at the rear end of the payload, pointing approximately  $90^\circ$  with respect to DXL. The DXL/STORM instrument is a prototype wide field-of-view soft X-ray camera using newly-developed micropore reflector technology. The instrument is designed for heliophysics, astrophysics, and planetary physics applications. The flight on DXL will represent the first time this technology will have been used to image the solar wind interaction with the terrestrial magnetosphere. The details of the DXL/STORM are reported elsewhere in this volume (Collier et al. 2012), in this paper we will focus on the DXL instrument.

For the scan we have chosen a region sufficiently close to the galactic plane to absorb soft X-rays produced outside the solar system and its local environment (within  $\sim 100 \text{ pc}$ ), therefore minimizing the intensity and structure of the cosmic background, as indicated by the Rosat All-Sky Survey (RASS). The DXL payload is scheduled to launch from White Sands Missile Range in New Mexico around 2012 December to ensure a scan path through the He focusing cone when the Sun is close to the maximum of its 11 year cycle.

### 2.1 The helium focusing cone

The bulk of the soft X-ray emission comes from SWCX with three neutral populations: interstellar hydrogen, interstellar helium, and the exospheric (geocoronal) hydrogen. SWCX due to geocoronal hydrogen may generate strong “bursts” of X-ray emission, which are clearly identifiable in X-ray observations. The flow of interstellar neutrals through the solar system is due to the motion of the heliosphere (at about  $25 \text{ km s}^{-1}$ ) through the local interstellar cloud (LIC). This material, a gas of mostly hydrogen atoms with about 15 % helium, flows from the direction of  $l \sim 252^\circ$ ,  $b \sim 9^\circ$ .

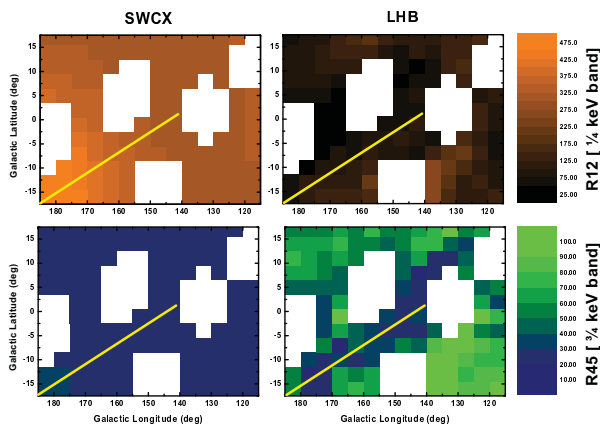


**Fig. 3** (online colour at: [www.an-journal.org](http://www.an-journal.org)) Expected contribution, in RU, of LHB and SWCX in the 1/4 keV (R12) and 3/4 keV (R45) energy bands with the mission scan path (yellow line).

This places the Earth upstream of the Sun in the interstellar neutral flow in early June and downstream in early December every year (Gruntman 1994).

Interstellar hydrogen experiences gravitational force, an almost equal repulsive force due to radiation pressure, and significant ionization due mainly to charge exchange with high speed solar protons (e.g., Quémerais et al. 1999; Lallement 1999), creating a hydrogen cavity around the sun. X-ray emission due to SWCX with interstellar hydrogen shows little geometric variation (dependence on location and look direction). However, only gravity significantly affects the helium trajectories which therefore execute Keplerian orbits and form a “focusing cone” downstream of the Sun centered at  $\sim 6^\circ$  below the ecliptic plane, resulting in a localized downstream enhancement of helium observed annually by Earth orbiting and L1 spacecrafts (Bzowski et al. 1996; Frisch 2000). The cone has a FWHM opening angle of about  $25^\circ$  and at one AU its density peaks at  $\sim 0.075 \text{ cm}^{-3}$  compared to a more typical value of  $\sim 0.015 \text{ cm}^{-3}$ . The peak density drops with distance from the Sun with a value of  $\sim 0.05 \text{ cm}^{-3}$  at 5 AU.

## 2.2 Observing strategy

The last solar maximum, solar cycle 23, occurred in 2001. The DXL payload will be launched from White Sands Missile Range in New Mexico during the month of December 2012 allowing a scan path through the He focusing cone when the sun is close to the maximum of its 11 year cycle.

The DXL observing strategy is based on the following guidelines:

- Launch in early December when the He focusing cone is aligned with the Sun-Earth line, directly opposite the Sun.
- Limit the scan to  $\pm 20^\circ$  from the galactic plane to assure that only “local” emission is detected ( $< 100 \text{ pc}$ ). This

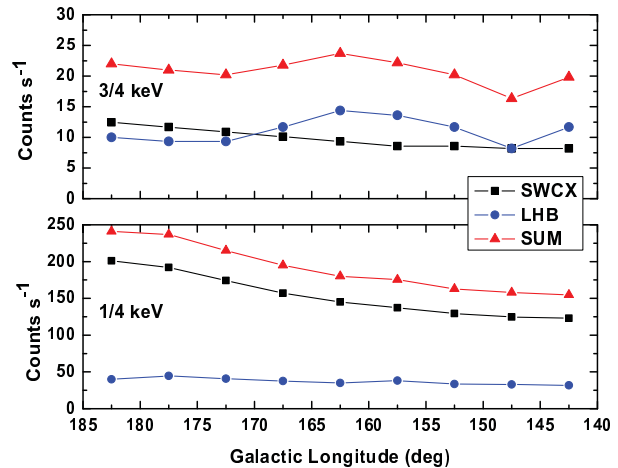


**Fig. 4** (online colour at: [www.an-journal.org](http://www.an-journal.org)) Expected DXL count rates in the 1/4 keV and 3/4 keV energy bands across the DXL scanning path due to LHB and SWCX emission.

will remove any contribution from diffuse X-ray components other than LHB and SWCX.

- The low galactic latitude will also avoid bright high latitude emission regions visible in the RASS maps.
- Avoid significantly bright point sources.
- Scan a region of the sky where the LHB emission is expected to be relatively uniform.

For the first DXL investigation we have chosen a region of the sky roughly centered at  $l \sim 150^\circ$ ,  $b \sim 0^\circ$ , shown in Fig. 3. The figure shows the expected contribution from the LHB and the SWCX in the 1/4 and 3/4 keV bands. The LHB contribution is calculated using RASS maps from which we subtracted our model of the SWCX for the RASS observing period and geometry, the SWCX contribution is calculated using our model for DXL geometry at solar maximum (Koutroumpa et al. 2006, 2007). Notice that, due to the different observing geometry, the RASS observations of this region were not significantly affected by the He focusing cone enhancement. The empty pixels correspond to regions with bright objects. The effect of the He focusing cone is clearly evident in the lower left corner of the 1/4 keV SWCX map and corresponds to an enhancement of about a factor of 2 in the SWCX emission. The green lines in the figures correspond to the chosen scan path.

The observation will start roughly in the direction of the He focusing cone, at  $l = 185^\circ$ ,  $b = -18^\circ$ , move to  $l = 140^\circ$ ,  $b = 0^\circ$  and back. During the observation, in the 1/4 keV band the SWCX emission is expected to be the biggest component and change from about  $300 \times 10^{-6} \text{ counts s}^{-1} \text{ arcmin}^{-2}$  (RASS Units, RU from now on) to more than 500 RU, while the remaining DXB emission should be roughly constant at 100 RU. In the 3/4 keV band the SWCX emission should change from about 20 RU to about 30 RU, while the remaining DXB should be roughly constant at about 30 RU. The combination of spatial information in the two separate bands should allow a clear sep-

aration and characterization of both components. The DXL count rate in both bands as a function of galactic longitude is shown in Fig. 4.

Assuming resolution elements of  $6^\circ \times 6^\circ$ , equal to the DXL resolution, a 5 minute flight will provide about 40 s observing time per resolution element, or between 6000 and 10 000 counts per resolution element in the 1/4 keV band and about 800 counts per resolution element in the 3/4 keV band, providing very high statistics for the data analysis. We note that we do not expect our count rate to be affected by any bright point source which will stay clear of our aperture. We also expect to have post-flight pointing accuracy of about one degree, which would allow us to use RASS to quantify and remove any such contribution in case the actual trajectory is significantly off the expected one.

### 2.3 Data analysis and expected results

The signal that DXL will measure is the sum of the SWCX emission due to the solar wind interactions with He and H, and the cosmic background emission. By observing in the downstream direction of the interstellar neutral flow we minimize both the total contribution and the spatial variation of the hydrogen SWCX. The total helium SWCX intensity  $I$  is the integral over the line of sight  $ds$  of the product of the solar wind density  $n_{sw}$ , the He density  $n_{He}$ , and the compound interaction cross-section  $\alpha$ :

$$I = \int \alpha n_{sw} n_{He} \langle g \rangle ds, \quad (1)$$

where  $\langle g \rangle$  is the averaged total solar wind speed (both bulk and thermal). The compound cross-section is the abundance weighted sum of the cross-sections of all the different species and ionization states in the solar wind. The individual cross-sections are velocity dependent and are poorly known, even for some of the dominant species.

The Advanced Composition Explorer (ACE) satellite (Stone et al. 1998) provides many of the important solar wind abundances and ionization state fractions for the solar wind as it passes the Earth. Combining the ACE data with a model of the solar wind we will reconstruct the solar wind density, velocity, and, more roughly, the ionization structure along the line of sight as a function of time. The shape of the profile in Fig. 4 is determined by the solar wind parameters and the distribution of the neutral He, both of which are reasonably well understood. The amplitude of the profile is instead determined by  $\alpha$ , which is not well understood.

As a first step, by fitting our observed profile with the solar wind and He models we can determine  $\alpha$ . By simultaneous fitting of DXL data and the ROSAT all-sky survey data (together with the IMP-8 solar wind data<sup>1</sup>) we can constrain the free parameters of the solar wind model, such as the latitude extent of the equatorial component of the solar wind. We then use the models and the newly determined values of  $\alpha$  to remove the He SWCX from the RASS. With a

better understanding of the SWCX parameters we will also repeat the several historic analyses that constrained the nature of the LHB to determine its properties if, in fact, there is still emission not accounted for by SWCX.

We note that, in our model, we have additional spectral information, that treats individually each ionization state, although in the 1/4 keV the uncertainties on the cross-sections may be large, as well as the various line emission probabilities. We will therefore also be working on the shape of the spectrum in the 1/4 keV, which is critical to determine the emission mechanism.

### 3 The instrument

The DXL payload consists of two thin-windowed, large area proportional counters mounted on an aluminium frame and supported by the rocket skin. The counters use a wire-wall design (multi-anode proportional counters with wire cathode walls) and are filled with P10 gas (90 % argon, 10 % methane) at 760 Torr. The X-rays are mechanically collimated using 2.5 cm thick, 3 mm cell honeycomb providing a circular field of view of  $6.5^\circ$  FWHM. Ceramic magnets embedded in the collimator provide a magnetic field of 150 Gauss within and above the collimators which intercepts electrons that could either generate scattered X-rays or mimic X-ray events in the detectors. A three-sided veto for cosmic-ray rejection is also obtained using anodes at the sides and back of each main counter.

One side of each counter, facing the mechanical collimators, is covered with a thin X-ray plastic window (25 cm  $\times$  50 cm, 80–90 mg cm<sup>-2</sup>) supported by a 100 lines-per-inch nickel mesh (with  $\sim 68\%$  transmission) to retain the counter gas while allowing soft X-ray photons to enter the counter. The windows are composed of Formvar (C<sub>5</sub>H<sub>7</sub>O<sub>2</sub>, the registered trade name of the poly-vinyl formal resin produced by Monsanto Chemical Company) with an additive, Cyasorb UV-24 (C<sub>14</sub>H<sub>12</sub>O<sub>4</sub>, a trade name of American Cyanamide), to absorb stellar ultraviolet photons that could otherwise generate a large non-X-ray background. The same windows were used for the DXS experiment (Sanders et al. 2001) that flew on-board the Space Shuttle Endeavour in January 1993. Geometrical effects, including the shadow of the nickel mesh, anticoincidence detectors, collimators, magnets, and masks near the ends of the anode wires reduce the effective area of each detector to about 600 cm<sup>2</sup>. The effective area as a function of energy, including the window transmission, is shown in Fig. 2 for the sum of both counters. While the energy resolution of the proportional counters is relatively poor below 1 keV, the carbon edge at 0.285 keV in the filter response allows a clear separation of the events below 1 keV in two different bands, corresponding roughly to the ROSAT 1/4 keV and 3/4 keV bands.

To ensure gain stability, a constant gas density is maintained inside the counters during the flight by using on-board gas bottles and pressure regulators. The regulators are

<sup>1</sup> <http://science.nasa.gov/missions/imp-8/>

true density regulators, using differential pressure between the main counter and a reference volume at the same temperature. A high-stability, high-voltage power supply provides 1700 V bias for the counters. Two  $^{55}\text{Fe}$  calibration sources (one for each counter) with mechanical shutters allow gain calibration during the flight.

The signal from the proportional counters is read out using low noise charge amplifiers, digitized, and telemetered to the ground. X-ray pulse heights are telemetered with a resolution of about 2 eV from 30 eV to 1 keV and 20 eV from 1 keV to 10 keV. The energy resolution is therefore limited by the intrinsic resolution of the proportional counters and is equal to about  $15 \times \sqrt{E[\text{eV}]}$  FWHM. A second set of multiple threshold discriminators also provides an estimate of the pulse amplitude as a backup for the main pulse acquisition system.

#### 4 Beyond the first flight

DXL is designed for a long term campaign for the investigation of the properties and characteristics of the LHB and SWCX, with additional flights beyond 2012. As noted before, our SWCX model, and in general any proper interpretation of SWCX emission, require additional spectral information by treating each ionization state individually. However, in the 1/4 keV band the uncertainties on the cross-sections, as well as the various line emission probabilities, may be large. The proportional counters on DXL do not have the energy resolution necessary to separate the lines generated by the various ionization states. However, additional energy information can be obtained by using different “filters” in front of the counters. For example, it is possible to replace the (mostly carbon) window in front of the counters with either a boron or a beryllium window to investigate different energy bands in the 1/4 keV range (see, e.g., McCammon & Sanders 1990, Fig. 3). The DXL payload is being designed with the necessary infrastructure to accommodate, in future flight(s), a smaller, 150 cm<sup>2</sup> counter capable of accommodating either a Be or B window, based on the counter design used by Bloch et al. (1986). It will then be possible to use detailed data from ACE for each ion species to separate the different ion contributions.

Moreover, although heliospheric SWCX is the primary concern for future X-ray missions, a good understanding of SWCX mechanisms requires also a study of its magnetosheath component. Magnetosheath SWCX is somewhat less than the heliospheric component, but may become the dominant term during periods of high solar wind flux. The X-ray emission due to magnetosheath SWCX is also affected by a significant spatial variation, with the brightest emission coming from the subsolar location (see, e.g., Porter et al. 2008). Such a spatial variation can be used, similarly to what has been described in this paper, to separate magnetosheath SWCX from other X-ray contributions to the DXB. The emission is significantly affected by the solar wind strength and composition, and the investigation

requires a launch synchronized with solar wind activity. Solar wind data are provided by ACE and available, in almost real time, through NOAA<sup>2</sup>. As solar wind activity cannot be predicted in advance, the investigation requires a continuous monitoring of ACE data while waiting for the proper solar wind conditions. Such a wait may last for days and it is not feasible from White Sands Missile Range due to the high cost and limited availability of launch dates. However, “the Sounding Rocket Program is planning to provide launches from Woomera, Australia, in the fall of calendar year 2014 and again in the spring of calendar year 2016, subject to the availability of funds” (ROSES-10 Amendment 26). Launching outside a military facility, with significantly smaller requirements, would be the perfect opportunity for such a triggered observation. A natural follow-up to the first DXL flights could therefore be two additional triggered flights from Woomera, one during a period of high solar wind flux, the other during an “average” period.

*Acknowledgements.* The investigation is supported by the National Aeronautics and Space Administration (NASA), grant # NNX11AF04G. The authors would like to thank the Engineering support at the University of Miami for the contribution in refurbishing the DXL payload.

#### References

- Bloch, J.J., et al.: 1986, *ApJ* 308, L59  
 Bzowski, M., et al.: 1996, *Icarus* 124, 209  
 Collier, M.R., et al.: 2012, *AN* 333, 378  
 Cox, D.P.: 1998, in: D. Breitschwerdt, M.J. Freyberg, J. Trümper (eds.), *The Local Bubble and Beyond*, IAU Coll. 166, LNP 506, p. 121  
 Cravens, T.E.: 1997, *Geophys. Res. Lett.* 24, 105  
 Cravens, T.E., et al.: 2001, *J. Geophys. Res.* 106, 24883  
 Frisch, P.C.: 2000, *J. Geophys. Res.* 105, 10279  
 Galeazzi, M., et al.: 2007, *ApJ* 658, 1081  
 Galeazzi, M., et al.: 2011, *Exp. Astr.* 32, 83  
 Gruntman, M.A.: 1994, *J. Geophys. Res.* 99, 19213  
 Gupta, A., et al.: 2009 *ApJ* 707, 644  
 Koutroumpa, D., et al.: 2006, *A&A* 460, 289  
 Koutroumpa, D., et al.: 2007, *A&A* 475, 901  
 Koutroumpa, D., et al.: 2009, *ApJ* 697, 1214  
 Lallement, R.: 1999, in: S.R. Habbal, C.D. Halas (eds.), *The solar wind nine conference*, AIPC 471, p. 205  
 Lallement, R.: 2004a, *A&A* 418, 143  
 Lallement, R.: 2004b, *A&A* 422, 391  
 McCammon, D., Sanders, W.T.: 1990 *ARA&A* 28, 657  
 McCammon, D., et al.: 2002, *ApJ* 576, 188  
 Porter, F.S., et al.: 2008, in: M.J.L. Turner, K.A. Flanagan (eds.), *Space Telescopes and Instrumentation 2008: Ultraviolet to Gamma Ray*, SPIE 7011, p. 70111L  
 Quémerais, E., et al.: 1999, *J. Geophys. Res.* 104, 12585  
 Robertson, I.P., Cravens, T.E.: 2003a, *J. Geophys. Res.* 108, 8031  
 Robertson, I.P., Cravens, T.E.: 2003b, *Geophys. Res. Lett.* 30, 1439  
 Sanders, W.T., et al.: 2001, *ApJ* 554, 694  
 Snowden, S.L., et al.: 2009, *ApJ* 691, 372  
 Stone, E.C., et al.: 1998, *Space Sci. Rev.* 86, 1

<sup>2</sup> <http://www.swpc.noaa.gov/SWN/index.html>